Catalysis Science & Technology

ROYAL SOCIETY OF CHEMISTRY

PAPER

View Article Online
View Journal | View Issue

Cite this: *Catal. Sci. Technol.*, 2023, **13**, 5017

Insights into Pt–CN species on an alumina-supported platinum catalyst as active intermediates or inhibitors for low-temperature hydrogen cyanide synthesis from methane and nitric oxide†

Atsushi Takagaki, *[a] Kyoko K. Bando, *[b] Tatsuya Yamasaki,[c] Junichi Murakami,[b] Nobuya Suganuma,[d] I. Tyrone Ghampson,[d] Tetsuya Kodaira,[e] Tatsumi Ishihara[cf] and Tetsuya Shishido *[dg]

Received 28th April 2023,
Accepted 24th July 2023

DOI: 10.1039/d3cy00581j

rsc.li/catalysis

Methane (CH_4) was converted to hydrogen cyanide (HCN) at temperatures from 300 to 425 °C using a commercial 5 wt% Pt/Al_2O_3 catalyst with nitric oxide (NO) as an oxidant. HCN yield of *ca.* 1% was maintained after 100 h at 400 °C, whereas the yield was increased to 3.2% at 425 °C but rapidly decreased, resulting in 0.24% after 90 h at 425 °C. *In situ* X-ray absorption fine structure (XAFS) and Fourier-transform infrared (FTIR) measurements showed that Pt–CN species emerged and the extent of the adsorbed species roughly correlated with the production of HCN. However, the Pt–CN species continuously accumulated at higher temperatures than 400 °C regardless of the catalytic activity. The experiment of purging using helium gas followed by hydrogen after the reaction of CH_4 and NO at 425 °C showed that the Pt–CN species were strongly adsorbed on the Pt catalyst and removed from the catalyst by hydrogen treatment with simultaneous formation of HCN and NH_3. This study revealed that the Pt–CN species can function not only as important reaction intermediates, but also as inhibitors of the reaction. An appropriate balance of Pt–CN species and hydrogen species over the Pt surface is required to produce HCN continuously.

Introduction

The CH_4–NO reaction has been investigated a few decades ago as a deNO_x reaction in which CH_4 was used as a reductant like H_2 and NH_3.[1–3] Pt catalyst could selectively convert hazardous NO in the low concentration (ppm level) to harmless N_2 along with the formation of CO_2. Recently, low-temperature activation of CH_4 has been attracting attention from both academic and industrial fields because of increasing demand for avoiding the use of fossil fuels.[4,5] The cleavage of the C–H bond at low temperature usually requires strong oxidant reagents such as H_2O_2 in liquid-phase reactions,[6,7] and NO/O_2 (NO/NO_2 oxygen atom shuttle) in gas-phase reactions,[8,9] or the use of non-thermal plasma,[10,11] while a representative exception is the system over Cu–zeolite using molecular oxygen as an ideal oxidant.[12–14]

We found that the use of NO as a sole oxidant in the presence of a Pt/Al_2O_3 catalyst afforded the selective production of hydrogen cyanide (HCN) from CH_4 at relatively low temperatures from 300 to 425 °C.[15,16] The production rate of HCN was 11.4 mmol g^{-1} h^{-1} and the corresponding turnover frequency was 253 h^{-1}, which was much higher than that of the plasma-assisted HCN synthesis method using a Pt/titanosilicate (TS-1) catalyst from CH_4 and NH_3 (17.6 h^{-1}).[17] The Pt/Al_2O_3 catalyst was able to have a high durability of 100 h and over when the reaction was carried out at 400 °C. While Pt-based catalyst (Pt–Rh gauze) is used for the industrial production of HCN through Andrussow and BMA

[a] *Division of Materials and Chemical Engineering, Faculty of Engineering, Yokohama National University, 79-5 Tokiwadai, Hodogaya-ku, Yokohama, Kanagawa 240-8501, Japan. E-mail: takagaki-atsushi-gw@ynu.ac.jp*
[b] *Nanomaterials Research Institute, National Institute of Advanced Industrial Science and Technology (AIST), 1-1-1, Higashi, Tsukuba, Ibaraki 305-8565, Japan. E-mail: k.k.bando@aist.go.jp*
[c] *Department of Applied Chemistry, Faculty of Engineering, Kyushu University, 744 Motooka, Nishi-ku, Fukuoka 819-0395, Japan*
[d] *Department of Applied Chemistry for Environment, Graduate School of Urban Environmental Sciences, Tokyo Metropolitan University, 1-1 Minami-osawa, Hachioji, Tokyo 192-0397, Japan. E-mail: shishido-tetsuya@tmu.ac.jp*
[e] *Research Institute for Chemical Process Technology, National Institute of Advanced Industrial Science and Technology (AIST), 1-1-1, Higashi, Tsukuba, Ibaraki 305-8565, Japan*
[f] *International Institute for Carbon-Neutral Energy Research (WPI-I²CNER), Kyushu University, 711 Motooka, Nishi-ku, Fukuoka 819-0395, Japan*
[g] *Elements Strategy Initiative for Catalysts and Batteries, Kyoto University, 1-30 Goryo-Ohara, Nishikyo-ku, Kyoto 615-8245, Japan*

† Electronic supplementary information (ESI) available: XRD, TEM, product yields as a function of temperature. See DOI: https://doi.org/10.1039/d3cy00581j

(Blausäure aus Methan und Ammoniak) processes operated at high temperature over 1000 °C,[18,19] the reaction mechanism of our study is different from that of the industrial processes because negligible formation of HCN was observed from a reaction of CH_4 with NH_3 and O_2 using Pt/Al_2O_3 at low temperature.[15] We previously claimed from the results of *in situ* FTIR/mass spectroscopy (MS) and *in situ* XAFS measurements that adsorbed Pt–CN species on platinum is attributable to an intermediate species for the production of HCN because the dependence of corresponding adsorption observed for both FTIR and XAFS spectra on the reaction temperature roughly correlated with that of the activity. However, a more detailed study for the Pt–CN species was necessary to understand the reactivity of Pt/Al_2O_3 for the low-temperature synthesis of HCN. In the present report, the behaviour of the adsorbed species including Pt–CN was monitored using *in situ* FTIR and XAFS measurements from 300 to 425 °C in a CH_4–NO gas atmosphere together with MS measurements for the detection of gaseous products. The influence of He and H_2 purge after the reaction at 425 °C on the reactivity of the adsorbed species was also conducted to clarify the role of the species. In addition, the long-term stability of the Pt/Al_2O_3 catalyst was studied at 400 and 425 °C and the significant difference of the results was discussed.

Experimental

Materials

The alumina-supported platinum catalyst (5 wt% Pt/Al_2O_3) was purchased from FUJIFILM Wako Pure Chemical. The reaction gases comprising CH_4 (99.9%), 10.4% NO in He, and He (99.9%) for the reactivity study were purchased from Fukuoka Oxygen Co., Ltd, and the gases used for *in situ* XAFS and FTIR measurements were obtained from Japan Fine Products. These gases were mixed to use as necessary.

Characterization

The physicochemical properties of the catalysts were evaluated according to our previous study.[15] The crystal structure was determined by X-ray diffraction (XRD, RINT-2500HLR+, Rigaku), and the specific surface area was evaluated with nitrogen adsorption (BELSORP mini-II, Microtrac BEL). The particle size distribution of Pt nanoparticles was observed using transmission electron microscopy (JEM-ARM200, JEOL).

Reactivity test

The low-temperature HCN synthesis reaction was conducted under ambient pressure using a fixed-bed continuous flow reactor. 100 mg of the Pt/Al_2O_3 catalyst was used, which was pelletized, crushed, and sieved to a particle size of 315–630 μm. Prior to each experiment, the catalyst was pretreated at 400 °C for 1 h under a flow of 50% H_2/He (100 mL min^{-1}). After the pretreatment, the gas was switched to He, and the reactor was set to the desired temperature. After stabilizing the desired temperature for 30 min, the reaction gas comprising 13.4% CH_4, 1.8% NO, and 84.8% He was fed to the reactor at a total flow rate of 100 mL min^{-1}. The reaction temperature was varied from 300 to 425 °C with 25 °C increments. The gaseous products were analysed by two on-line gas chromatographs (GCs) and one Fourier transform infrared (FTIR) spectrometer. Several products including HCN, CH_3CN, CO, CO_2, NH_3, N_2, N_2O and H_2O were detected in addition to the reactants, CH_4 and NO. The first GC (Nexis GC-2030, Shimadzu) equipped with a barrier discharge ionization detector (BID) together with a capillary column (Restek, Rt-U-BOND, 30 m × 0.53 mm i.d. × 20 μm film diameter) was used for the analysis of CO_2, H_2O, HCN and CH_3CN. The second GC (GC-2014, Shimadzu) with a thermal conductivity detector (TCD) and a molecular sieve column (MS-13X, 2 m × 3 mm i.d.) was employed for the analysis of O_2, N_2 and CH_4. The on-line FTIR spectrometer (VIR-200, JASCO) equipped with a triglycine sulphate (TGS) detector together with a 10 cm gas cell was used to analyse NO, NO_2, N_2O, NH_3, and CO. The FTIR spectra were taken at a resolution of 1 cm^{-1} over the range from 7800 to 800 cm^{-1}. Quantitative analysis was based on a calibration curve prepared using a reference gas of known composition. Conversion and yield were calculated using the equations provided below. Here, n_i is the number of moles of i at the exit of the reactor, $n_{i,0}$ is the moles in the feed, and v_i is the number of carbon or nitrogen atoms in species i.

$$\text{CH}_4\ \text{conversion}\ (\%) = \left(1 - \frac{n_{\text{CH}_4}}{n_{\text{CH}_4,0}}\right) \times 100$$

$$\text{NO conversion}\ (\%) = \left(1 - \frac{n_{\text{NO}}}{n_{\text{NO},0}}\right) \times 100$$

$$\text{Yield (carbon based)}\ (\%) = \frac{v_i n_i}{n_{\text{CH}_4,0}} \times 100$$

$$\text{Yield (nitrogen based)}\ (\%) = \frac{v_i n_i}{n_{\text{NO},0}} \times 100$$

Caution: This experiment requires special attention because of the highly toxic HCN generated. Always make sure that there are no leaks from the gas line or the reaction apparatus and monitor them with a gas sensor.

In situ XAFS/MS

In situ XAFS and MS measurements were carried out in the BL9C beamline of the Photon Factory at the Institute of Materials Structure Science, High-Energy Accelerator Research Organization (KE-IMSS-PF, proposal nos. 2019G070 and 2020G039). The mass spectrometer (BELMASS, MicrotracBEL) was employed to analyse the gas products. 100 mg of the Pt/Al_2O_3 powder was pressed into a disc with a

diameter of 10 mm, and set in an *in situ* reactor equipped with Kapton windows which were cooled by circulating water. Pt L_3-edge XAFS spectra were measured in the transmission mode using ionization chambers for the detection of primary (I_0, 15% Ar/N_2) and transmitted (I_T, 50% Ar/N_2) X-ray. The *in situ* XAFS measurement was carried out in a quick mode with a 60 s acquisition time per spectrum over an energy range of 11 057–12 661 eV. The composition, and flow rate of the reactant gas and the temperature in the catalyst pretreatment and reaction were the same as those in the reactivity test using the fixed-bed reactor. The spectra of Pt foil and PtO_2 were taken as references in a step scan mode and the spectrum of Pt foil was used for energy calibration. Data processing was performed using Athena software ver.0.9.26.[20]

In situ FTIR

In situ FTIR measurement was performed to monitor the behaviour of adsorbed species on the catalyst surface after the reaction followed by hydrogen treatment at 425 °C. An FTIR spectrometer (FT/IR-610, JASCO) equipped with a mercury cadmium telluride (MCT) detector was used. A self-supporting disc with a diameter of 10 mm comprising 15 mg Pt/Al_2O_3 was placed in an *in situ* stainless cell equipped with KBr windows which were kept at 25 °C by circulating cooling water. The relative gas composition, and flow rate of the reactant gas and the temperature in the catalyst pretreatment and reaction were the same as those in the reactivity test using the fixed-bed reactor.

Results and discussion

The alumina-supported platinum catalyst (5 wt% Pt/Al_2O_3) used in this study consists of Pt particles with an average particle size of 4.3 nm and alumina that is primarily in the γ phase with a partial θ phase with a surface area of 99 $m^2\ g^{-1}$.

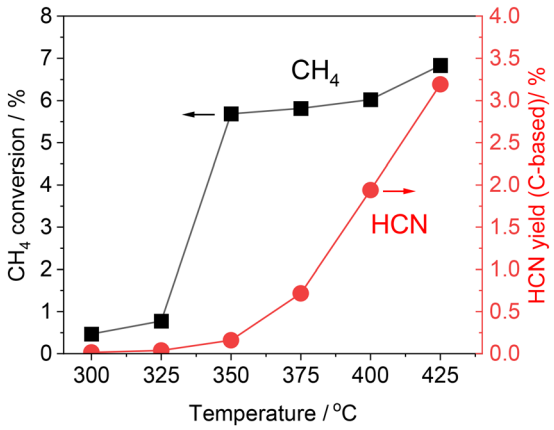

Fig. 1 Methane conversion and hydrogen cyanide yield (carbon-based) as a function of temperature for the reaction of methane with nitric oxide over the Pt/Al_2O_3 catalyst. Reaction conditions: 5 wt% Pt/Al_2O_3 (100 mg), $CH_4:NO:He$ = 13.4 : 1.8 : 84.8 (total flow rate: 100 mL min^{-1}), and 0.1 MPa.

The XRD pattern and TEM image of the sample are shown in Fig. S1 (see ESI†). In our previous study, the reactivity was evaluated by increasing temperature from 300 to 425 °C (Fig. 1 and S2†).[15] After introduction of the reactant gas at 300 °C, 0.02% of HCN carbon-based yield was obtained, indicating that C–H cleavage, NO dissociation, and C–N coupling reactions occurred at such low temperature. The increase of reaction temperature increased the HCN yield which reached 3.2% at 425 °C. Note that the CH_4 conversion increased markedly from 350 °C, and at 350 °C and 375 °C, most of the product was fully oxidized CO_2 (Fig. S2†). Thereafter, the yield of CO_2 decreased, and at 400 °C, the yields of HCN and CO_2 were about the same, and at 425 °C, the yield of CO_2 decreased to about 1/3 of that of HCN. The long-term stability has been confirmed at 400 °C for 100 h. Although the HCN yield at 400 °C was initially 1.9% and decreased during the early stages of the reaction, it gradually became steady and reached 0.92% after 100 h. As the initial yield of HCN was higher at 425 °C than at 400 °C, long-term tests were also conducted at 425 °C in the present study.

Fig. 2 shows the results of the long-term durability of the catalyst at 400 and 425 °C in terms of product yields. Both

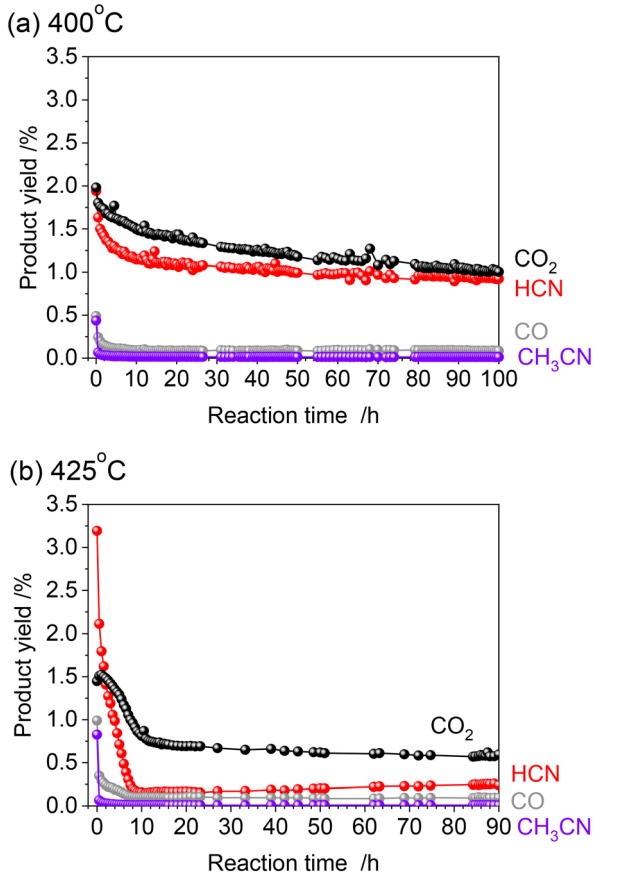

Fig. 2 Time-course of the reaction for methane with nitric oxide over the Pt/Al_2O_3 catalyst at 400 °C (a) and 425 °C (b). Reaction conditions: 5 wt% Pt/Al_2O_3 (100 mg), $CH_4:NO:He$ = 13.4 : 1.8 : 84.8 (total flow rate: 100 mL min^{-1}), and 0.1 MPa.

experiments were conducted after introducing CH_4 and NO starting at 300 °C and increasing the temperature in 25 °C steps in the same manner. As mentioned above, at 425 °C, the initial HCN yield was 3.2%, much higher than at 400 °C. However, a significant decrease in the HCN yield was observed, which was quite different from the long-term test at 400 °C. The HCN yield decreased considerably to 0.15% after 12 h. Interestingly, however, as the reaction was prolonged, the HCN yield gradually increased, reaching 0.24% after 90 h. More than 20 points were measured from 12 to 90 h of reaction, and the yield of HCN increased steadily with time. This suggests that the adsorbed species on the active site changes dynamically during the reaction.

After the long-term reaction, the spent catalysts were taken from the reactor and exposed in air. Fig. 3 shows the *ex situ* Pt L_3-edge XANES spectra of the spent catalysts after the reaction at 400 and 425 °C along with the spectra of Pt foil and PtO_2 as references. The intensity of the white line in the XANES spectra of the spent catalyst was weak and closer to that of Pt foil than that of PtO_2. In addition, none of the spectra of the spent catalysts were represented by a linear combination fitting of Pt and PtO_2. Fig. 3 also shows the difference in XANES spectra of the spent catalyst and that of the Pt foil. Both spent catalysts for the reaction at 400 and 425 °C showed similar spectra. Negative absorptions were observed at 11 562 eV whereas positive ones at 11 569 eV, indicating that the energy was shifted due to the formation of adsorbed species on the catalyst surface. In our previous study, the increase of absorbance at 11 569 eV (Δ7 eV from E_0) was attributed to the adsorption of Pt–CN species.[15] Because this absorbance at 11 569 eV became stronger with reaction temperature in the *in situ* measurement, we assumed that this Pt–CN species was the active species in the reaction. However, in the present study, the difference XANES spectrum of the catalyst reacted at 425 °C, where deactivation was observed, appears to be similar to that of the spent catalyst reacted at 400 °C, where HCN was steadily produced, suggesting that this Pt–CN species is not merely contributing as an active species.

These results motivated us to investigate *in situ* XAFS/MS measurements from 300 to 450 °C because in the previous study the XAFS and MS measurements were carried out separately and the *in situ* XAFS measurement was examined from 300 to 400 °C and the data above 400 °C were lacking.[15] Fig. 4 shows the *in situ* XAFS/MS spectroscopy result for the reaction of CH_4 and NO over the Pt/Al_2O_3 catalyst. The reaction temperature was increased by 25 °C increments from 300 to 450 °C. Each temperature was held for 60 min and then raised to the next temperature at a rate of 5 °C min^{-1}. Eight mass signals corresponding to NO and several products including HCN are shown together with the Pt L_3-edge XAFS absorbance at 11 569 eV characteristic of the Pt–CN species. At the initial stage of the reaction at 300 °C, the mass signal of 30 (m/z = 30) corresponding to NO was very small and increased to a certain level with time, indicating that most of NO was quickly adsorbed on the catalyst and reacted to form N_2O (m/z = 44) or N_2 (m/z = 28). The N_2O signal was initially quite high but rapidly decreased, which is in good agreement with the increased NO signal (*i.e.* decreased NO conversion). The Pt L_3-edge XAFS absorbance at 11 569 eV also rapidly increased, and then continued to increase gradually at 300 °C. When the temperature was increased to 325 °C, the MS signal for NO decreased, indicating that more NO gas reacted. The MS signal for N_2O (and CO_2) (m/z = 44) increased again then gradually decreased, but substantially higher than that at 300 °C, which is in good agreement with the increase of N_2O yield at 325 °C in our previous reactivity test.[15] The MS signal of HCN (m/z = 27) apparently increased, indicating the formation of HCN at the temperature. The intensity of the corresponding XANES spectra monotonically increased from 300 to 325 °C. Thereafter, the MS signal for NO (m/z = 30)

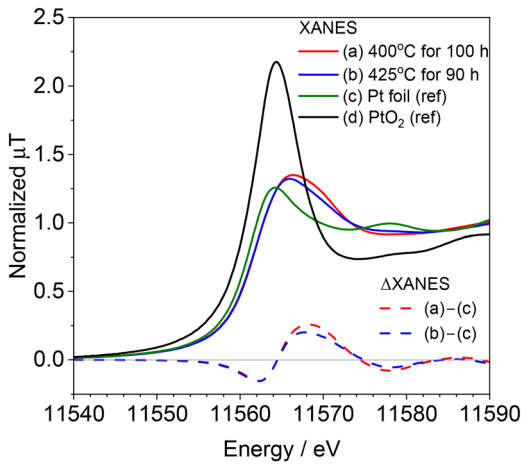

Fig. 3 Pt L_3-edge XANES spectra of the Pt/Al_2O_3 catalyst after the reaction with methane and nitric oxide at 400 °C for 100 h or 425 °C for 90 h, and the difference XANES spectra of the spent catalysts and Pt foil.

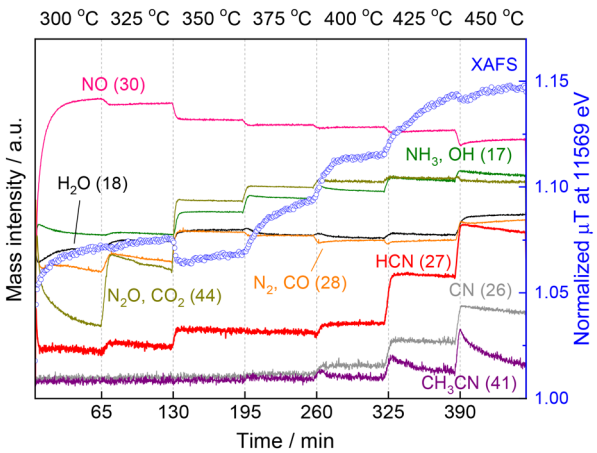

Fig. 4 Changes of the MS spectra and the XAFS intensity (at 11 569 eV) at various temperatures raising from 300 to 450 °C with 25 °C steps. Reaction conditions: 5 wt% Pt/Al_2O_3 (100 mg), CH_4 : NO : He = 13.4 : 1.8 : 84.8 (total flow rate: 100 mL min^{-1}), and 0.1 MPa.

decreased stepwise with increasing reaction temperature, consistent with the increase in NO conversion in the reactivity test. From 350 °C, the formation of NH_3 and CO_2 was pronounced, and the corresponding MS signals (m/z = 17 and 44) also increased. The XANES absorbance decreased once at 350 °C and then increased again. In the previous study,[15] at lower temperature a distinct peak was observed at 11 568 eV, which was attributed to Pt–CO.[21,22] This suggests that the increase in 11 569 eV at 300 and 325 °C is mainly due to the adsorbed species of Pt–CO. The apparent decrease of the XANES absorbance at 11 569 eV from 325 to 350 °C could be due to the change of adsorbed species from Pt–CO to Pt–CN on the Pt surface. The same result was obtained for another experiment of temperature-programmed reaction as shown below. At 375 °C, the XANES absorbance increased with time, suggesting the accumulation of Pt–CN species on the catalyst surface. When the temperature was increased to 400 °C, the XANES absorbance increased markedly with increasing the MS signal for HCN. However, after about 15 min, the XANES intensity became almost constant and simultaneously the MS signal for HCN (m/z = 27) remained unchanged. At 425 °C, the MS signal for HCN increased further, and at the same time the MS signal for CH_3-CN (m/z = 41) clearly increased. Thereafter, the MS signal for HCN gradually decreased with time. On the contrary, the absorbance of XANES increased monotonically, which is much different from the mostly constant absorbance at 400 °C. When the reaction temperature was further raised to 450 °C, the MS signal for HCN increased again with the signal for CH_3CN, but these signals clearly decreased with the reaction time, indicating the deactivation of the catalyst at such high temperature. The XANES absorbance at 11 569 eV decreased slightly once only when the temperature was increased from 425 to 450 °C, but continued to increase after reaching 450 °C, indicating that Pt–CN species accumulated on the catalyst surface. These results show that although the HCN production and XANES absorbance increased with increasing reaction temperature, the HCN production and XANES absorbance did not necessarily coincide at temperatures above 425 °C. Rather, the catalytic activity was found to decrease with increase in the XANES absorbance, which is associated with an increase in Pt–CN adsorbed species.

Next, another *in situ* XAFS/MS experiment was performed in which the reaction was carried out by raising the temperature to 425 °C, followed by hydrogen treatment and then the reaction was implemented again. The temperature and gas time profiles along with the MS spectra are shown in Fig. 5. Prior to the reaction with CH_4 and NO, the catalyst was pretreated by H_2 at 400 °C for 1 h the same as our previous study. After switching H_2 to He with cooling to 300 °C, the reaction with CH_4 and NO started at 300 °C for 30 min, then the temperature was increased to 425 °C at the rate of 10 °C min^{-1} as the temperature-programmed reaction (TPR). Afterward, the temperature was kept at 425 °C for 30 min in the presence of CH_4 and NO. At the same temperature, the gas was changed to He for 30 min to remove the reaction gas from the cell, and then H_2 was introduced for 1 h. After 30 min of He purging, the CH_4 and NO reaction gas

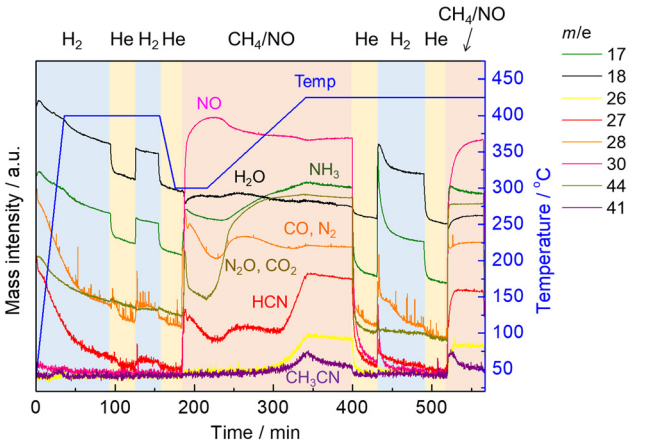

Fig. 5 The time profiles of operating temperature, the gas composition, and the obtained MS spectra.

was introduced again isothermally. Changes of the MS spectra during TPR showed the same trend as in the previous experiment with stepwise temperature changes. It should be noted that the MS signal for HCN (m/z = 27) increased significantly from 400 to 425 °C but decreased with time at 425 °C, which is in good agreement with the previous experiment. After switching to He, all MS signals decreased with time, indicating the removal of the reaction gas from the cell. After the He purging, the treatment with H_2 allowed the desorption of HCN and NH_3, suggesting that some adsorbed species (likely Pt–CN) on the catalyst surface, which could not be removed by He purging, reacted with hydrogen to form HCN and NH_3. When the reaction gas composed of CH_4 and NO was introduced again after the He purging, the MS signals for products including HCN, NH_3 and CH_3CN increased with a rapid consumption of NO at the initial stage of the reaction.

The XANES difference spectra measured simultaneously with the MS spectra are shown in Fig. 6. At 300 and 325 °C, the spectra were broad, but at temperatures above 350 °C, the peak attributable to Pt–CN species was clearly observed and increased in intensity with temperature (Fig. 6(a)). It should be noted that the peak at 11 569 eV is assigned to the Pt–CN species in the present study, but this is a simple assumption because the shape of the spectra implies that it contains multiple components, and the intensity of the spectrum does not exactly match that of the Pt–CN species observed in the FTIR measurement. Although we do not exclude the possibility that other adsorbed species or structural changes of the catalyst during the reaction may also contribute, the present study mainly discusses the behaviour of the Pt–CN species. At 425 °C, the peak continued to increase with time (Fig. 6(b)) while the MS signal for HCN slightly decreased shown in Fig. 5. When the atmosphere was changed from the reaction gas to He, the peak of ΔXANES spectra decreased very slightly but substantially remained unchanged, indicating that the Pt–CN species were strongly adsorbed on the catalyst surface at 425 °C (Fig. 6(c)). After the introduction of H_2, the peak rapidly

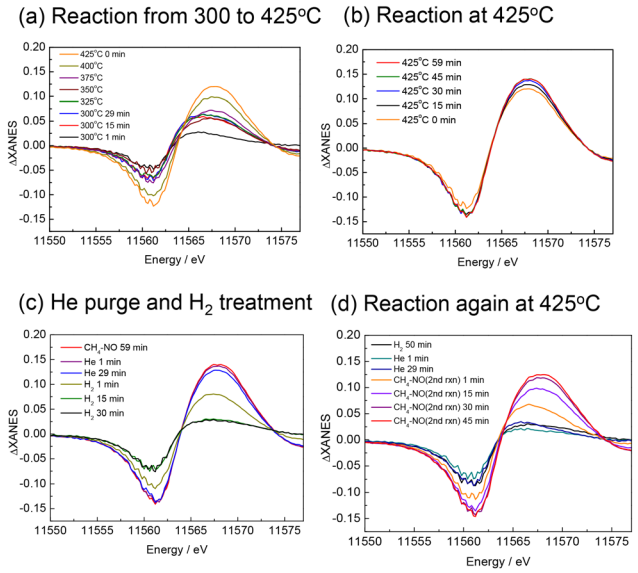

Fig. 6 Pt L_3-edge XANES difference spectra subtraction of the spectrum just before the introduction of CH_4 and NO mixture. (a) Reaction from 300 to 425 °C, (b) reaction at 425 °C, (c) He purge and H_2 treatment after the first reaction at 425 °C, (d) the second reaction at 425 °C after He purge and H_2 treatment.

decreased to almost zero, indicating the full removal of the adsorbed species. This is consistent with the formation of HCN and NH_3 desorbed from the catalyst surface. After He purging followed by the introduction of the reaction gas, the peak at the same position was recovered and increased with prolonged time (Fig. 6(d)). Note that in Fig. 6(d) the peak top of the spectrum of the second reaction after 1 min (coloured in orange) is different from the others. It appears similar to those at the begging of the first reaction at 300 °C (Fig. 6(a)). The CO and N_2 signals in the MS also rose immediately after the initial introduction of CH_4–NO gases, indicating that Pt–CO was also formed at the beginning of the second reaction.

A similar experiment that reacted with CH_4 and NO at 425 °C followed by He purge and hydrogen treatment was examined by *in situ* FTIR. Fig. 7 shows the *in situ* FTIR spectra at 425 °C, which was measured in a transmission mode using a Pt/Al_2O_3 self-supporting disc set in a stainless reactor. The reaction was carried out by introducing CH_4 and NO at 300 °C followed by increasing the reaction temperature to 425 °C. The strong absorption was observed at 2148 cm^{-1}, which is attributed to Pt–CN species.[23] When hydrogen was flowed into the reactor after He purging, the adsorption peak was decreased with time, indicating the removal of adsorbed Pt–CN species. This result is in a good agreement with that of the *in situ* XAFS/MS measurement. Another experiment was carried out by the fixed bed flow reactor and the on-line FTIR spectrometer with a 10 cm gas cell. The experimental conditions were the same as the *in situ* XAFS/MS and *in situ* FTIR measurements.

Fig. 8 shows the results of products including HCN, NH_3, N_2O and CO which were detected by FTIR every two minutes. When the gas was switched from a mixture of CH_4 and NO to He at 425 °C, the concentration of CO increased sharply and then decreased, indicating the removal of Pt–CO species from the catalyst surface by He purging. It should be noted that while the concentrations of HCN and NH_3 were very low in the He flow, those were clearly increased by H_2 treatment. This experiment further confirmed that the strongly adsorbed Pt–CN species were removed by H_2 resulting in the formation of HCN and NH_3. The amount of HCN desorbed was calculated to be 0.58 μmol by integration. The amount of active sites of the Pt catalyst was 43 μmol g^{-1}.[15] As 100 mg of the catalyst was used for the reaction, the amount of HCN desorbed corresponded to 13% of the amount of the Pt surface sites. The results of long-term tests at 400 and 425 °C were described above in which the total amount of HCN formed by 90 h reaction at each temperature was 30.5 and

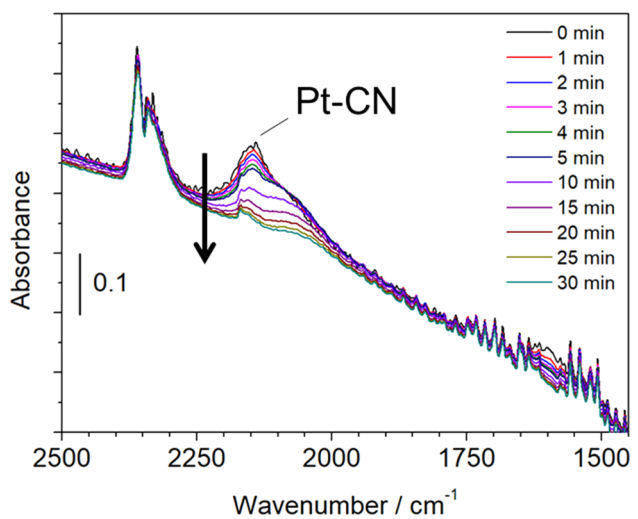

Fig. 7 *In situ* FTIR spectroscopy results for the reaction of CH_4 and NO followed by He purge and hydrogen treatment on the Pt/Al_2O_3 catalyst at 425 °C. Time (min) indicates that treated with hydrogen.

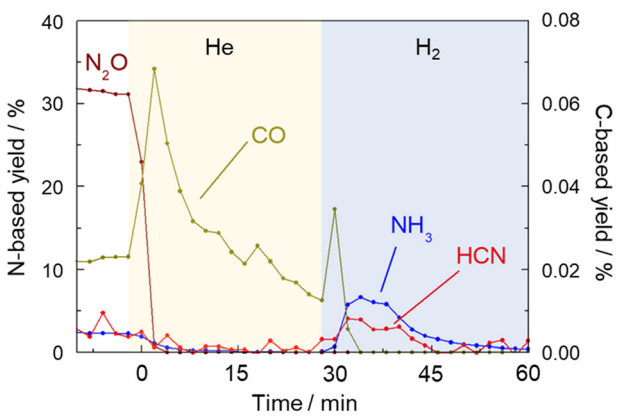

Fig. 8 Yields of gaseous products (HCN (C-based), CO (C-based), N_2O (N-based), and NH_3 (N-based)) determined by FTIR spectroscopy during the reaction CH_4–NO (before 0 min), He purging (0–28 min), and H_2 treatment (after 28 min).

8.0 mmol, respectively. From these values, turnover number was 7100 and 1860 at 400 and 425 °C, respectively, reconfirming that HCN was more stably formed at 400 °C. The steady yield of HCN at 400 °C was 0.92%, which corresponds to the production rate of 50 μmol g^{-1} min^{-1} and TOF of 1.2 min^{-1}. In contrast, the yield of HCN at 425 °C for 90 h was 0.24%, indicating TOF of 0.3 min^{-1}. Considering that the amount of HCN desorbed comes from Pt–CN species adsorbed on the Pt catalyst, it is difficult to discuss the 13% coverage quantitatively, but this value is not necessarily off the mark, since the hydrogen species formed by methane cleavage, the NO-derived active oxygen species to cleave the C–H bonds of that methane, and even the nitrogen species for C–N coupling should all be on the same Pt surface.

We have previously reported the effect of the particle size of Pt on the HCN formation.[16] The HCN yield was higher for Pt catalysts with larger Pt particles under the same contact time. The XAFS results of four spent Pt catalysts of different particle sizes showed that the peak at 11 569 eV assigned to Pt–CN was observed for all Pt catalysts, but the absorption intensity was higher for the smaller Pt catalysts with lower HCN yield and lower for the larger Pt catalyst with higher HCN yield. This result is consistent with the conclusion of the present study that Pt–CN adsorbed species are both active and inhibitor species.

Conclusions

The Pt–CN species were formed during the reaction with CH_4 and NO and continued to be accumulated at high temperature, which caused the decrease of catalytically active sites of Pt. The Pt–CN species were strongly adsorbed on the catalyst surface which could not be removed in He purge. The introduction of hydrogen helped to desorb the species resulting in the formation of gaseous HCN and NH_3 as products. Thus, the lack of hydrogen species on the catalyst surface would be a major reason for deactivation of the catalyst at temperatures higher than 425 °C. In the present reaction conditions, the only hydrogen source is CH_4 in which the C–H bond is cleaved by oxidation using active oxygen species which are delivered by dissociative adsorption of NO. The Pt catalysts are capable to catalyse multiple reactions including dissociation of NO, activation of CH_4 and formation of Pt–CN species as well as desorption of HCN in which these reactions proceed on the same active sites. The Pt–CN species are the key intermediate species to produce HCN, but because of the strong adsorption property, the species continue to be accumulated on the active sites of the catalyst when hydrogen supply *via* CH_4 cleavage is not enough. Therefore, the Pt–CN species are not only the intermediates but also behave as inhibitors. The continuous production of HCN requires an appropriate balance of Pt–CN species *via* C–N coupling and hydrogen species *via* C–H cleavage over the Pt surface.

Author contributions

AT, KB and TS: conceptualization; AT, KB, TY, JM, NS, ITG and TK: investigation and methodology; KB and TS: formal analysis; AT, KB, IT and TS: supervision; AT, KB and TS: funding acquisition; AT: writing – original draft; KB, ITG, TK and TS: writing – review & editing.

Conflicts of interest

There are no conflicts to declare.

Acknowledgements

This work was supported by the Japan Science and Technology (JST) Agency under the CREST program, Grant Number JPMJCR16P2. A part of this work was performed at the KEK-IMSS-PF (2019G070 and 2020G039).

Notes and references

1 R. Burch and S. Scire, *Appl. Catal., B*, 1994, **3**, 295–318.
2 R. Burch and A. Ramli, *Appl. Catal., B*, 1998, **15**, 49–62.
3 I. Balint, A. Miyazaki and K.-I. Aika, *Chem. Commun.*, 2002, 1044–1045.
4 H. Fujisaki, T. Ishizuka, H. Kotani, Y. Shiota, K. Yoshizawa and T. Kojima, *Nature*, 2023, **616**, 476–481.
5 Z. Liang, T. Li, M. Kim, A. Asthagiri and J. F. Weaver, *Science*, 2017, **356**, 299–303.
6 C. Hammond, M. M. Forde, M. H. Ab Rahim, A. Therford, Q. He, R. L. Jenkuns, N. Dimitratos, J. A. Lopez-Sanchez, N. F. Dummer, D. M. Murphy, A. F. Carley, S. H. Taylor, D. J. Willock, E. E. Stangland, J. Kang, H. Hagen, C. J. Kiely and G. J. Hutchings, *Angew. Chem., Int. Ed.*, 2012, **51**, 5129–5133.
7 P. K. Sajith, A. Staykov, M. Yoshida, Y. Shiota and K. Yoshizawa, *J. Phys. Chem. C*, 2020, **124**, 13231–13239.
8 V. Vargheese, J. Murakami, K. K. Bando, I. T. Ghampson, G.-N. Yun, Y. Kobayashi and S. T. Oyama, *J. Catal.*, 2020, **389**, 352–365.
9 I. T. Ghampson, S.-T. B. Lundin, T. Shishido and S. T. Oyama, *Catal. Sci. Technol.*, 2021, **11**, 2708–2712.
10 T. Nozaki and K. Okazaki, *Catal. Today*, 2013, **211**, 29–38.
11 W. Bi, Y. Tang, X. Li, C. Dai, C. Song, X. Guo and X. Ma, *Commun. Chem.*, 2022, **5**, 124.
12 S. Grundner, M. A. C. Markovits, G. Li, M. Tromp, E. A. Pidko, E. L. M. Hensen, A. Jentys, M. Sanchez-Sanchez and J. A. Lercher, *Nat. Commun.*, 2015, **6**, 7546.
13 K. Narsimhan, K. Iyoki, K. Dinh and Y. Román-Leshkov, *ACS Cent. Sci.*, 2016, **2**, 424–429.
14 V. L. Sushkevich, D. Palagin, M. Ranocchiari and A. A. van Bokhoven, *Science*, 2017, **356**, 523–527.
15 T. Yamasaki, A. Nishida, N. Suganuma, Y. Song, X. Li, J. Mukarami, T. Kodaira, K. K. Bando, T. Ishihara, T. Shishido and A. Takagaki, *ACS Catal.*, 2021, **11**, 14660–14668.
16 T. Yamasaki, A. Takagaki, T. Shishido, K. K. Bando, T. Kodaira, J. Murakami, J. T. Song, E. Niwa, M. Watanabe and T. Ishihara, *J. Jpn. Pet. Inst.*, 2022, **65**, 184–191.

17 Z. Guo, Y. Yi, L. Wang, J. Yan and K. Guo, *ACS Catal.*, 2018, **8**, 10219–10224.
18 V. A. Kondratenko, G. Weinberg, M.-M. Pohl and D. S. Su, *Appl. Catal., A*, 2010, **381**, 66–73.
19 D. Hasenberg and L. D. Schmidt, *J. Catal.*, 1986, **97**, 156–168.
20 B. Ravel and A. Newville, *J. Synchrotron Radiat.*, 2004, **12**, 537–541.
21 T. Kubota, K. Asakura and Y. Iwasawa, *Catal. Lett.*, 1997, **46**, 141–144.
22 O. V. Safonova, M. Tromp, J. A. van Bokhoven, F. M. F. de Groot, J. Evans and P. Glatzel, *J. Phys. Chem. B*, 2006, **110**, 16162–16164.
23 G. R. Bamwenda, A. Obuchi, A. Ogata and K. Mizuno, *Chem. Lett.*, 1994, **23**, 2109–2112.